Optical Engineering

SPIEDigitalLibrary.org/oe

# Method to transmit analog information by using a long distance photonic link with distributed feedback lasers biased in the low laser threshold current region

Alejandro García-Juárez
Ignacio E. Zaldívar-Huerta
Jorge Rodríguez-Asomoza
María del Rocío Gómez-Colín

# Method to transmit analog information by using a long distance photonic link with distributed feedback lasers biased in the low laser threshold current region

**Alejandro García-Juárez**
Universidad de Sonora
Departamento de Investigación en Física
C. P. 83000, Hermosillo, Sonora, México
E-mail: agarcia@cifus.uson.mx

**Ignacio E. Zaldívar-Huerta**
Instituto Nacional de Astrofísica Óptica y Electrónica
Departamento de Electrónica
Apdo. Postal 51 y 216
Puebla, C. P. 72000, México

**Jorge Rodríguez-Asomoza**
Universidad de las Américas-Puebla
Departamento de Ingeniería Electrónica
Ex-hacienda Sta. Catarina Mártir, Cholula
Puebla, C. P. 72820, México

**María del Rocío Gómez-Colín**
Universidad de Sonora
Departamento de Física
C. P. 83000, Hermosillo, Sonora, México

**Abstract.** We describe an analog microwave photonic link system, which is used to transmit in a multiplexed way a TV signal over 30 km of standard optical fiber. The experimental setup is composed mainly by two distributed feedback (DFB) laser diodes emitting at 1500 nm. When these DFB lasers are operated in the low laser threshold current region, relaxation oscillation frequencies are obtained. Relaxation oscillations in the laser intensity can be seen as sidebands on both sides of the main laser line. The optical emissions generated in each laser are combined and amplified by using an erbium-doped fiber amplifier. Next, the amplified optical signal is detected by a fast photo-detector using direct detection method, and as result of this photo-detection, microwave signals are generated. Since microwave signals obtained by using this technique are tuned continuously; we can use them as electrical carriers to transmit simultaneously a TV signal at 4 and 5 GHz and over 30 km of standard optical fiber by using a Mach-Zehnder modulator. At the end of the optical link the modulated light is photo-detected in order to recover efficiently and successfully the analog TV signal.  [DOI: 10.1117/1.OE.51.6.065006]

Subject terms: relaxation oscillation frequency; threshold current; distributed feedback laser; direct detection; intensity modulation-direct detection systems; microwave photonics; microwave generation; microwave carriers.

Paper 120008P received Jan. 2, 2012; revised manuscript received Apr. 6, 2012; accepted for publication May 14, 2012; published online Jun. 8, 2012.

## 1 Introduction

Currently, several companies are involved in the transport of radio frequency (RF) or microwave signals over fiber-optic radio links. Radio over fiber (RoF) links are considered as a promising technique in providing broadband wireless access services in the emerging optical-wireless networks. The modulation scheme that decides the way to generate the optical millimeter-wave signal is a key technique in this optical-wireless access networks architecture.[1–3] The simplest RoF system consists of a central site (CS) and a remote site (RS) connected by an optical fiber link or network. The frequencies of the radio signals distributed by RoF systems span a wide range (usually in the GHz region), and the applications for such systems range from in-building distribution of wireless signals (for example, in shopping malls and tunnels), wireline interconnections between base stations and microcellular antennas, antenna remoting for various commercial (wing-tip antennas in aircraft) and military radar systems, and broadcasting of cable television signals in both hybrid fiber coax (HFC) and triplexer based fiber-to-the-home (FTTH) systems.[4] On the other hand, a traditional RF photonic link operating at 1550 nm consists of a directly modulated distributed feedback (DFB) laser diode (LD), a length of fiber-optic transmission medium, and a photodetector (PD).[5] The fiber chromatic dispersion intrinsically occurring in standard 1550-nm single-mode fibers (SMFs) is one of the main drawbacks that limit the transmission distance and operation bandwidth of such RF fiber-optic systems. However, if low dispersion fiber is used in conjunction with an appropriate choice of the laser operating parameters, the system becomes quasi-linear.[6] DFB lasers are the proper light sources for these applications because of their single longitudinal mode, with side-mode suppression ratio (SMSR) in the order of 40 dB and stable operation with a narrow spectral width, but the characteristic relaxation oscillations peak in the laser intensity, which produces sidebands on both sides of the main laser line, imposes a limiting factor on the proximity of two channels in a communication system. Besides, relaxation oscillations limit the high-frequency response of semiconductor lasers and the sensitivity in low-frequency applications. In order for an optical analog transmission of GHz-range signal to be successful in RoF systems, it is necessary to have a good DFB laser without their inherently serious problem of the modulation distortion caused by several factors [spatial-hole burning (SHB), leakage current, nonlinear interaction of carriers and photons, gain compression, nonlinear I-V characteristics in a p-n heterojunction, and power-dependent absorption] and including relaxation oscillations frequencies. We recently demonstrated this when a DFB laser biased in the low laser threshold current region showed relaxation oscillation frequencies in the laser intensity.[7] These frequencies were seen as sidebands on both sides of the main laser line when the optical spectrum was analyzed with a spectrum analyzer. This result allowed the generation of microwave signals on C band

0091-3286/2012/$25.00 

using direct detection method. Besides with the proposed experimental setup in that work, an analog National Television System Committee (NTSC) TV signal was transmitted and received satisfactorily in a short distance wireline communication system by using relaxation oscillation frequency as information carrier. In this paper we propose a microwave photonic link architecture to transmit simultaneously a TV signal at 4 and 5 GHz and over 30 km of standard optical fiber. In this case we have used two DFB laser diodes emitting at 1550 nm and operating in the low laser threshold current region. When the emissions generated in both lasers are combined by using an optical fiber coupler and detected by a fast photodetector using direct detection method, two microwave signals are obtained. These frequencies acting as information carriers were mixed with a TV signal. The signal obtained in the output of the mixer is imposed on an optical carrier of a DFB laser as an intensity modulation using a lithium niobate (LN) Mach—Zehnder intensity modulator (MZM). The modulated optical carrier was transmitted over 30 km of standard optical fiber. At the end of the link, a photodiode was used to convert the intensity modulation back to the microwave signals mixed with TV signals. After that, TV signals were recovered satisfactorily. The remainder of this paper is structured as follows. Theoretical description of the relaxation oscillation frequency based on a small signal modulation analysis is presented in Sec. 2.1. This theory is an additional contribution to the article submitted to Photonics West 2012.[8] The operation principle of direct detection is given in Sec. 2.2. An analytical description of a microwave photonic link by using external modulation is presented in Sec. 2.3. Signal-to-noise ratio (SNR) performance of an analog photonic link is described in Sec. 2.4. The proposed transmission system is explained in Sec. 3. Discussions are presented in Sec. 4. Finally, our conclusion to this work is provided in Sec. 5.

## 2 Theoretical Description

The organization of this section is divided into four subsections. First, we give a theoretical description of the relaxation oscillation frequency of a laser diode. Next, we describe the basic principle of operation of direct detection for measuring relaxation oscillation frequency. After that, we describe the operation principle of a photonic link based on external modulation. Finally, signal-to-noise ratio (SNR) performance of an analog photonic link is described.

### 2.1 *Theoretical Description of the Relaxation Oscillation Frequency*

The relaxation oscillation frequency is the frequency of the quasi-sinusoidal oscillations about the steady-state output power amplitude that occur during the disturbance of a continuously operating laser. Such oscillations are characterized by exponential damping. The phenomenon of relaxation oscillations has an effect on the performance of an unmodulated laser as well, by producing sidebands in the field fluctuation spectrum. They may be found directly from a small-signal measurement. Figure 1 illustrates the typical standard setup that is used for characterization of laser diodes. We assume that the laser diode is excited by an AC current source with amplitude and electrical frequency $\omega$, biased at the constant current $I_0$ by means of a bias-tee. The modulated laser output is coupled into an optical fiber

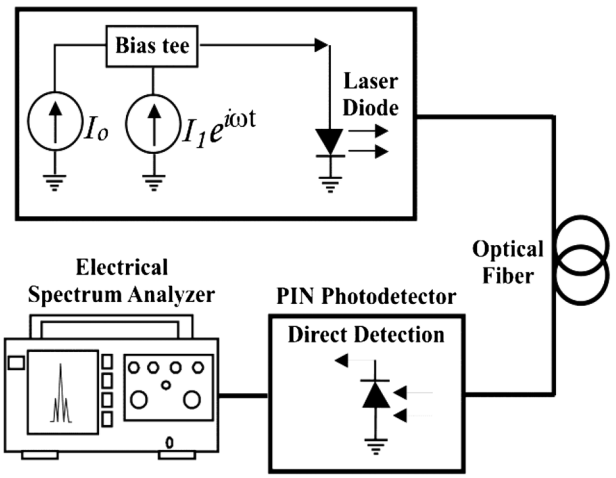


**Fig. 1** Typical experimental setup for measurement of relaxation oscillation frequencies of laser diodes.

and then into a semiconductor PIN diode, biased through a simple bias network. The detected signal is fed into a spectrum analyzer.

#### 2.1.1 *Analysis of relaxation oscillation frequency*

The employed physical model for analyzing the harmonic power can be explained by considering the small signal modulation analysis where the total electric current injected into the laser diode is given by:

$$I = I_0 + I_1 e^{j\omega t}. \tag{1}$$

If photon and electron densities inside the active region of a semiconductor laser are denoted, respectively, by $N_P$ and $N_E$, then expanding $N_P$ and $N_E$ as a Fourier series we obtain that these densities can be written as:

$$N_E = \sum_{n=0}^{\infty} N_{En} e^{jn\omega t}, \tag{2}$$

$$N_P = \sum_{n=0}^{\infty} N_{Pn} e^{jn\omega t}, \tag{3}$$

where $N_{Pn}$ and $N_{En}$ are the corresponding expansion coefficients of the photon and electron densities, respectively. On the other hand, the well-known rate equations for a single-mode laser diode are:[9]

$$\frac{dN_E}{dt} = \eta_i \frac{I}{qV} - \frac{N_E}{\tau_e} - V_g a(N_E - N_{\mathrm{tr}})N_P, \tag{4}$$

$$\frac{dN_P}{dt} = \Gamma V_g a(N_E - N_{\mathrm{tr}})N_P - \frac{N_P}{\tau_p}, \tag{5}$$

where $\eta_i$ is the efficiency coefficient, $\tau_e$ is the carrier lifetime, $a$ is the differential gain, $N_{\mathrm{tr}}$ is the threshold electron density, $\Gamma$ is the cavity confinement factor, $V_g$ is the cavity volume, and $\tau_p$ is the photon lifetime. In order to obtain information related with harmonic contents in optical output power of a laser diode, it is necessary to start our approach by substituting Eqs. (1) to (3) in Eq. (4), which results in:

$$j\omega\sum_{n=1}^{\infty}N_{E_n}ne^{jn\omega t}=\eta_i\frac{I_0+I_1e^{j\omega t}}{qV}-\frac{1}{\tau_e}\sum_{n=0}^{\infty}N_{E_n}e^{jn\omega t}-V_ga\left(\sum_{n=0}^{\infty}N_{E_n}e^{jn\omega t}-N_{\mathrm{tr}}\right)\times\sum_{n=0}^{\infty}N_{P_n}e^{jn\omega t}. \tag{6}$$

In a similar way, if we substitute Eqs. (2) and (3) in Eq. (5) we obtain:

$$j\omega\sum_{n=1}^{\infty}N_{p_n}ne^{jn\omega t}=\Gamma V_ga\left(\sum_{n=0}^{\infty}N_{E_n}e^{jn\omega t}-N_{tr}\right)\times\sum_{n=0}^{\infty}N_{P_n}e^{jn\omega t}-\frac{1}{\tau_p}\sum_{n=0}^{\infty}N_{p_n}e^{jn\omega t}. \tag{7}$$

From DC analysis (n = 0), however, we have:

$$N_{E_0}=\frac{\eta_i\frac{I_0}{qV}+V_gaN_{tr}N_{P_0}}{\frac{1}{\tau_e}+V_gaN_{P_0}} \tag{8}$$

$$\frac{1}{\Gamma\tau_p}=V_ga(N_{E_0}-N_{\mathrm{tr}}). \tag{9}$$

The first harmonic of the photon density is generated directly by the first harmonic of the current applied to the laser diode, and we easily obtain:[10]

$$N_{E_1}=\frac{\eta_i\frac{I_1}{qV}}{j\omega+\frac{1}{\tau_e}+V_gaN_{P_0}\left(1+\frac{1}{j\omega\tau_p}\right)} \tag{10}$$

$$N_{P_1}=\frac{\Gamma V_gaN_{P_0}}{j\omega}N_{E_1}. \tag{11}$$

Higher harmonics are found from recursive equations, which in the general case for an arbitrary integer, $k>1$, may be written as:

$$jk\omega N_{E_k}=-\frac{N_{E_k}}{\tau_e}-V_ga\left[(N_{E_0}-N_{\mathrm{tr}})N_{P_k}+N_{E_k}N_{P_0}+\sum_{n=1}^{k-1}N_{E_n}N_{P_{k-n}}\right] \tag{12}$$

$$jk\omega N_{P_k}=\Gamma V_ga\left(N_{E_k}N_{P_0}+\sum_{n=1}^{k-1}N_{E_n}N_{P_{k-n}}\right). \tag{13}$$

Hence, the $k$th harmonic of the photon density may be calculated, once all the lower harmonics of photon and electron densities are known. If we define $M_k$ as the parameter that relates the $k$th harmonic to the lower ones,[11]

$$M_k=\sum_{n=1}^{k-1}N_{E_n}N_{P_{k-n}}. \tag{14}$$

Therefore, we can find the $k$th harmonics of photon and electron densities as:

$$N_{E_k}=\frac{-V_ga\left(1+\frac{1}{jk\omega\tau_p}\right)}{jk\omega+\frac{1}{\tau_e}+V_gaN_{P_0}\left(1+\frac{1}{jk\omega\tau_p}\right)}M_k \tag{15}$$

$$N_{P_k}=\frac{\Gamma V_ga}{jk\omega}\left(N_{P_0}N_{E_k}+M_k\right). \tag{16}$$

The frequency, $\omega_{RO}$, at which the amplitude of the power harmonic content reaches its maximum is called the relaxation resonant frequency. From Eqs. (10) and (11), the primary harmonic of the photon density is obtained as:[10]

$$N_{P_1}=\frac{\Gamma V_gaN_{P_0}}{j\omega}\frac{\eta_i\frac{I_1}{qV}}{j\omega+\frac{1}{\tau_e}+V_gaN_{P_0}\left(1+\frac{1}{j\omega\tau_p}\right)}. \tag{17}$$

On the other hand, if the optical output power for the $k$th harmonic is given by $P_k=P_{\mathrm{out}_k}=\frac{hvV_p}{\tau_m}N_{p_k}$, where $\tau_m$ is the mirror loss time, $V_p$ represents the cavity volume and $hv$ is the energy per photon. Then, by using this last equation, we can obtain the optical output power for the first harmonic, which is written as:

$$P_1(j\omega)=\frac{hvV_p}{\tau_m}\left[\frac{\Gamma V_gaN_{P_0}\eta_i\frac{I_1}{qV}}{-\omega^2+\frac{j\omega}{\tau_e}+\frac{V_gaN_{P_0}}{\tau_p}(j\omega\tau_p+1)}\right]. \tag{18}$$

The cavity confinement factor, $\Gamma$, is equal to the ratio, $V/V_p$; therefore, the above can be written as:

$$\frac{P_1(j\omega)}{I_1(j\omega)}=\frac{hvV_gaN_{P_0}\eta_i\frac{1}{\tau_mq}}{-\omega^2+\frac{j\omega}{\tau_e}+\frac{V_gaN_{P_0}}{\tau_p}(j\omega\tau_p+1)}. \tag{19}$$

By separating the real and imaginary parts of the denominator of Eq. (19), we finally get:[11]

$$\frac{P_1(j\omega)}{I_1(j\omega)}=\frac{hvV_gaN_{P_0}\eta_i\frac{1}{\tau_mq}}{\frac{V_gaN_{P_0}}{\tau_p}-\omega^2+j\omega\left(\frac{1}{\tau_e}+V_gaN_{P_0}\right)}. \tag{20}$$

This expression clearly has two poles at:

$$\omega=\pm\left[\frac{1}{\tau_p}V_gaN_{P_0}-\frac{1}{4}\left(\frac{1}{\tau_e}+V_gaN_{P_0}\right)^2\right]^{\frac{1}{2}}+j\frac{1}{2}\left(\frac{1}{\tau_e}+V_gaN_{P_0}\right), \tag{21}$$

which are located in the first and second quadrants of the complex $\omega$ plane. We now notice that the real part of the denominator of Eq. (20) becomes zero at the frequency:

$$\omega=\omega_{RO}^2=\frac{V_gaN_{P_0}}{\tau_p}, \tag{22}$$

where $\omega_{RO} = 2\pi f_{RO}$ is called the Relaxation Resonant Frequency. Since usually $\frac{1}{\tau_p} + V_g a N_{P_0} \ll \omega_{RO}$ holds, we conclude that the magnitude of Eq. (20) also reaches a maximum when $\omega \approx \omega_{RO}$. Hence, the denominator becomes purely imaginary, and the primary power harmonic content reaches its resonance mode.

The optimum modulation frequency is the resonant frequency, which is determined from the bias current. Therefore, the optimal operation point for modulation where the power of the primary harmonic reaches its maximum must lie on the curve obtained from the following:[12]

$$\omega_{RO} = \sqrt{\frac{V_g a}{q V_p} \eta_i (I_0 - I_{\text{th}})}. \tag{23}$$

From the laser rate equations it is clear that the relaxation oscillation frequency should be proportional to the square root of the difference of the injection current and the threshold current. Thus, from Eq. (23) we can see that there is a linear relationship between relaxation oscillation frequency and the square root of the difference between the injection current and the threshold current. On the other hand, when the laser current density is lightly increased above its threshold value, the laser output power may be written as:[13]

$$P_o = \eta_d (I_{\text{in}} - I_{\text{th}}) \frac{1.24}{\lambda_o}, \tag{24}$$

where $\eta_d \frac{1.24}{\lambda_o}$ is called the differential responsivity of the laser (W/A).

### 2.2 *Operation Principle of Direct Detection*

When a laser is biased in the threshold current region as shown in Fig. 2, the laser intensity presents oscillations know as relaxation frequencies and can be seen as sidebands on both sides of the main laser line. In this case the electric field emitted by the laser diode can be represented as an optical signal directly modulated. The optical field incident on the photodetector after passing through an optical fiber can be expressed as:[7,8]

$$\begin{aligned} E(t) = {} & E_o \cos(2\pi f_o t) + E_{RO} \cos 2\pi (f_o + f_{RO}) t \\ & + E_{RO} \cos 2\pi (f_o - f_{RO}) t, \end{aligned} \tag{25}$$

where $f_o$ is the optical frequency of the main laser line, both $f_o + f_{RO}$ and $f_o - f_{RO}$ represent optical sidebands. This method of detecting optical fields as shown in Fig. 1 is called direct detection. The photodetector responds to the power in the total field that it collects. The photocurrent generated in the detector is proportional to the squared magnitude of the field and it is given by:[14]

$$i(t) = \Re |E(t)|^2 = \Re P(t), \tag{26}$$

where $P(t)$ is the optical power and $\Re$ is the detector responsivity given by:[14]

$$\Re = \frac{\eta q}{h\upsilon} [A/W], \tag{27}$$

where $\eta (0 < \eta \leq 1)$ is the detector quantum efficiency, a measure of the conversion efficiency of incident photons into electrical charge. The parameters $q$ and $h\upsilon$ are electronic charge ($1.6021 \times 10^{-19}$ C) and photon energy ($h = 6.6256 \times 10^{-34}$ J, $\upsilon = c/\lambda$), respectively. Substituting Eq. (25) into Eq. (26), and by using trigonometric identities, we obtain:

$$\begin{aligned} i(t) = {} & \Re |E_o \cos(2\pi f_o t) \\ & + E_{RO} [\cos 2\pi (f_o + f_{RO}) t + \cos 2\pi (f_o - f_{RO}) t]|^2 \\ = {} & \frac{E_o^2}{2} + E_{RO}^2 + \frac{E_o^2}{2} \cos^2 2\pi (2 f_o t) \\ & + 2 E_o E_{RO} \cos 2\pi (f_{RO}) t \\ & + E_o E_{RO} [\cos 2\pi (2 f_o + f_{RO}) t + \cos 2\pi (2 f_o - f_{RO}) t] \\ & + \frac{E_{RO}^2}{2} \cos 2\pi (2 f_o + 2 f_{RO}) t \\ & + E_{RO}^2 [\cos 2\pi (2 f_o) t + \cos 2\pi (2 f_{RO}) t] \\ & + \frac{E_{RO}^2}{2} \cos 2\pi (2 f_o - 2 f_{RO}) t. \end{aligned} \tag{28}$$

Notice that there are many terms in the detected signal expression where the photodetector cannot follow currents that are varying at $2f_o$, $2f_o + f_{RO}$, $2f_o - f_{RO}$, $2f_o + 2f_{RO}$ and $2f_o - 2f_{RO}$, so these currents average to zero. The average current from photodetector will consist of four terms:

$$\begin{aligned} i(t) = \Re \Big[ & \frac{E_o^2}{2} + E_{RO}^2 + 2 E_o E_{RO} \cos 2\pi (f_{RO}) t \\ & + E_{RO}^2 \cos 2\pi (2 f_{RO}) t \Big]. \end{aligned} \tag{29}$$

The photocurrent generated at the photodetector is found in a similar way as:

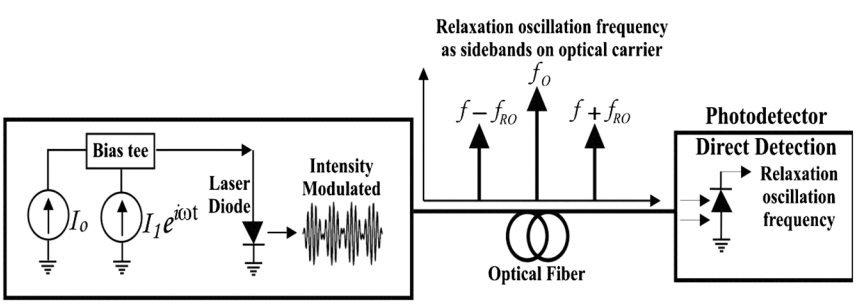


**Fig. 2** Direct detection to generate relaxation oscillation frequency when laser is operated in low threshold region.

$$i(t) = \Re\left[\frac{P_o}{2} + P_{RO} + 2\sqrt{P_o P_{RO}}\cos 2\pi(f_{RO})t + P_{RO}\cos 2\pi(2f_{RO})t\right]. \quad (30)$$

The first two terms correspond to DC photocurrents and contain no information, but they do contribute to the shot noise of the signal detected; the next two terms correspond to the signal information, which contains the relaxation oscillation frequency $f_{RO}$ and its harmonic located at $2f_{RO}$.

### 2.3 *Microwave Photonic Link by Using External Modulation*

The photonic link described in this section is shown in Fig. 3. The optical source is a continuous-wave DFB laser, followed by an erbium-doped fiber amplifier (EDFA). Amplified light is launched into the MZM. Microwave modulation is imposed on the optical carrier through the MZM. The modulated signal passes through of optical fiber and is then incident upon the photodetector. Photodetector output can be connected to a microwave spectrum analyzer to observe gain, noise figure, and distortion of the microwave signal obtained at the end of the link.

For a modulator with half-wave voltage of $V_\pi$, signal voltage $V$, input power $P_{\text{in}}$, and insertion loss $\alpha$, the modulated output power can be written:[15,16]

$$P_{\text{out}} = \frac{\alpha P_{\text{in}}}{2}\left[1 + \cos\left(\frac{\pi V}{V_\pi}\right)\right]. \quad (31)$$

This expression can be examined in more detail by separating the signal voltage into a DC bias, $V_b$, and a modulation voltage, $V_m$.

$$P_{\text{out}} = \frac{\alpha P_{\text{in}}}{2}\left[1 + \cos\left(\frac{\pi V_b}{V_\pi} + \frac{\pi V_m}{V_\pi}\right)\right]. \quad (32)$$

Using a trigonometric identity for the sum of cosines, the output power can be rewritten as:

$$P_{\text{out}} = \frac{\alpha P_{\text{in}}}{2}\left[1 + \cos\left(\frac{\pi V_b}{V_\pi}\right)\cos\left(\frac{\pi V_m}{V_\pi}\right) - \sin\left(\frac{\pi V_b}{V_\pi}\right)\sin\left(\frac{\pi V_m}{V_\pi}\right)\right]. \quad (33)$$

Typically, the DC bias point of the MZM is chosen to bring the modulator into quadrature. This is accomplished by operating at $V_b = V_{\pi/2}$. At this bias voltage, the transfer curve is linear and even order harmonics are suppressed.

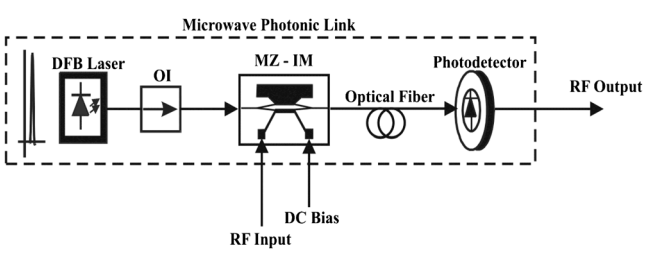


**Fig. 3** Microwave photonic link.

Deviation from the quadrature bias point can be described by an angle $\phi$.

$$P_{\text{out}} = \frac{\alpha P_{\text{in}}}{2}\left[1 + \cos\left(\frac{\pi}{2} + \phi\right)\cos\left(\frac{\pi V_m}{V_\pi}\right) - \sin\left(\frac{\pi}{2} + \phi\right)\sin\left(\frac{\pi V_m}{V_\pi}\right)\right] \quad (34)$$

$$P_{\text{out}} = \frac{\alpha P_{\text{in}}}{2}\left[1 - \sin\phi\cos\left(\frac{\pi V_m}{V_\pi}\right) - \cos\phi\sin\left(\frac{\pi V_m}{V_\pi}\right)\right]. \quad (35)$$

At $\phi = 0$, $V_b = V_{\pi/2}$ and the modulator is in quadrature. This corresponds to the typical linear transmission regime for an electro-optic modulator. The quadrature output power from the modulator is denoted by $P_Q$.

$$P_Q = \frac{\alpha P_{\text{in}}}{2}\left[1 - \sin\left(\frac{\pi V_m}{V_\pi}\right)\right]. \quad (36)$$

For single applications, the DC bias point of the MZM can be shifted away from the quadrature point. Even-order distortion is increased, but these terms lie outside the frequency range of interest. As the bias point is shifted, shot noise falls linearly with transmission and relative intensity noise (RIN) is reduced quadratically. However, the link gain is only reduced at the rate of $\sin^2\phi$. For links dominated by RIN, shifting the bias point toward the transmission null reduces the link noise figure. This improvement continues until the shot noise limit is reached.

Consider a MZM biased near $\phi = 90$ deg. This corresponds to an operating regime with reduced output power. For simplicity, let $\phi = 90$ deg $-\delta$ so that $\phi = 0$ deg corresponds to the quadrature operating point and $\delta = 0$ deg corresponds to the transmission null. These operating regimes and angles are summarized graphically in Fig. 4.

By substituting $\delta$ for $\pi/2 - \phi$, the modulator output power can be written as:[16]

$$P_{\text{out}} = \frac{\alpha P_{\text{in}}}{2}\left[1 - \cos\delta\cos\left(\frac{\pi V_m}{V_\pi}\right) - \sin\delta\sin\left(\frac{\pi V_m}{V_\pi}\right)\right]. \quad (37)$$

The first bracketed term represents continuous wave output power. The second term contains even-order harmonic components. The third term contains the linear signal of

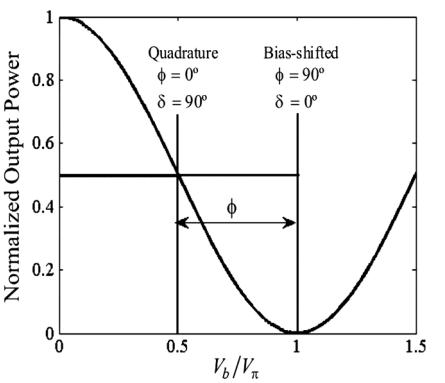


**Fig. 4** Quadrature and bias-shifted operating regimes.

interest as well as odd-order harmonic components. Note that for $\delta = 90$ deg, $P_{\text{out}} = P_Q$ as expected. For $\delta \ll 1$, the output power can be approximated by using a Taylor series expansion to replace sin $\delta$ with $\delta$ and cos $\delta$ with $1 - \delta^2/2$

$$P_{\text{out}} \approx \frac{\alpha P_{in}}{2}\left[1 - \left(1 - \frac{\delta^2}{2}\right)\cos\left(\frac{\pi V_m}{V_\pi}\right) - \delta \sin\left(\frac{\pi V_m}{V_\pi}\right)\right]. \tag{38}$$

The harmonic components can be identified by assuming small signal operation with $\pi V_m/V_\pi \ll 1$. For the cosine function, the Taylor series expansion can be truncated after the first term. This truncation is justified by operating the modulator over a single octave so that even-order distortion can be neglected.

$$P_{\text{out}} \approx \frac{\alpha P_{in}}{2}\left[1 - \left(1 - \frac{\delta^2}{2}\right) - \delta \sin\left(\frac{\pi V_m}{V_\pi}\right)\right]. \tag{39}$$

The sine term can be expressed using a third-order Taylor series expansion.

$$P_{\text{out}} \approx \frac{\alpha P_{\text{in}}}{2}\left\{\frac{\delta^2}{2} - \delta\left[\frac{\pi V_m}{V_\pi} - \frac{1}{6}\left(\frac{\pi V_m}{V_\pi}\right)^3 \cdots\right]\right\}. \tag{40}$$

From this expression, it can be seen that the DC term decreases more rapidly than the modulation term for a given increase in $\delta$. By shifting the DC bias point away from quadrature, carrier suppression can be achieved. This can create a double sideband suppressed carrier (DSB-SC) modulation format.

### 2.4 *SNR Performance of an Analog Photonic Link*

To reconstruct a signal at the receiver faithfully, the noise power must be small compared to the signal level. In other words, the SNR is a figure of merit in characterizing a receiver circuit. There are three dominant noise sources on the optical receiver side of an analog photonic link. Those are thermal and shot noises, and received RIN. In a photodetector, noise can be attributed primarily to two factors. The shot noise, also known as quantum noise, originates from the statistical nature of photon to electron conversion. Thermal noise, on the other hand, is an intrinsic property of any electrical circuit that is connected to the photodetector. The RIN is the fluctuations of the laser intensity caused by random spontaneous light emissions.

#### 2.4.1 *Shot noise*

Photon-to-electron conversion is fundamentally a quantum mechanical process. When a photon is absorbed, a pair of electron holes is generated. Therefore, the photo-generated current is not truly continuous, but has a discrete nature. It fluctuates around some average value as a result of the discrete charge of the carriers that contribute to it. Because of the random nature of the current fluctuations, the noise current must be characterized in a statistical manner. It is common to describe the noise current by its mean square value. For a PIN detector, the mean square value of the shot noise is:[17]

$$\sigma_s^2 = 2qI_P B, \tag{41}$$

where $I_P$ is the photocurrent, q is the electron charge, and $B$ is the bandwidth within which the noise is being measured. Equation (41) implies that shot noise has a constant spectral density, an assumption that holds for all frequencies of interest. Normally, $B$ is set by the bandwidth of the receiver. This shows that one way to minimize the effects of shot noise is to keep the bandwidth of circuit as narrow as possible. The current flowing through a PIN diode is not just photo-generated. Any reverse bias junction has a leakage current. For photodetectors the leakage current is called dark current $I_D$, because it exists even when these is no optical power. As a result, the mean square value of the total shot noise is given by

$$\sigma_s^2 = 2q(I_P + I_D)B. \tag{42}$$

#### 2.4.2 *Thermal noise*

Shot noise is a consequence of the quantum nature of light detection. Therefore, it is a fundamental property of the photodetector and sets a maximum limit on the value of SNR. In such a case, the SNR is said to be quantum limited. In reality, however, almost always there are other sources of noise present. Chief among these is thermal noise, also known as Johnson noise, associated with the electric circuits connected to the detector. The source of this noise is the thermal motion of electrons in the load resistor $R_L$. The mean squared of the thermal noise in the load resistor is given by

$$\sigma_T^2 = \frac{4kTB}{R_L}, \tag{43}$$

where $k$ is Boltzmann's constant, $T$ is the absolute temperature, and $B$ is bandwidth. Like shot noise, thermal noise has a constant spectral density. This is another reason to keep the bandwidth of a receiver as low as possible, that is, just sufficient to pass the signals of interest.

#### 2.4.3 *Relative intensity noise*

Any real laser has a certain amount of noise due to spontaneous emission. As a result both the amplitude and the phase are randomly varying in any real laser, then the wave front a DFB laser source may be represented by its electric field as

$$\bar{E}_1(t) = E_o[1 + V(t)] \exp\, j[2\pi v_o t + \varphi(t)], \tag{44}$$

where $V(t)$ and $\varphi(t)$ represent the amplitude and phase of the noise, respectively. If the field expressed in Eq. (44) is detected by a photodetector with responsivity $\mathfrak{R}$, the resulting current is given by:[18]

$$I = \mathfrak{R}E_o^2[1 + V(t)]^2. \tag{45}$$

Typically, the amplitude noise, $V(t)$, is very small, so that Eq. (45) can be rewritten as:

$$I \approx \mathfrak{R}E_o^2[1 + 2V(t)]. \tag{46}$$

The noise term $2V(t)$ represents the RIN; it describes the laser power fluctuations. The power spectral density of the RIN is denoted by $\zeta$; it has the units of $1/\text{Hz}$. The quantity $10 \log \zeta$ is known as the RIN

$$\mathrm{RIN} \equiv 10 \log \zeta, \qquad \mathrm{dB/Hz}. \tag{47}$$

The typical values of RIN for a DFB laser are better than −155 dB/Hz. The power spectrum of the RIN is not flat, hence it is not a white noise source. In an analog photonic link, we use a photodiode to detect the optical power from the M-Z modulator. Thus, RIN can be expressed as:[19]

$$\mathrm{RIN} = \frac{\left(\frac{i_{\mathrm{RIND}}}{\Re}\right)^2}{B\left(\frac{I_D}{\Re}\right)^2} = \frac{i^2 \mathrm{RIND}}{BI_D^2}. \tag{48}$$

From Eq. (48), we obtain the received mean square current RIN noise of the receiver as:

$$i_{\mathrm{RIND}}^2 = RIN \cdot I_D^2 B. \tag{49}$$

Comparing with the shot noise, $i_{\mathrm{RIND}}^2$ is proportional to $I_D^2$, whereas the shot noise is linearly proportional to $I_D$. Therefore, the RIN noise will tend to be the dominant noise, when the laser average power is increasing.

### 2.4.4 *Signal-to-noise ratio*

Once we have characterized the noise level at the input of a receiver, it is possible to analyze the SNR. The SNR is an important parameter because it determines the performance of a receiver. In analog receivers, SNR is the main figure of merit and characterizes the quality of the analog link. Assuming that all of the noise sources described previously are uncorrelated, the SNR of the link at the single photodetector can be expressed by:

$$\begin{aligned}\mathrm{SNR} &= \frac{\Re^2 P_R^2}{\sigma_s^2 + \sigma_T^2 + i_{\mathrm{RIND}}^2} \\ &= \frac{\Re^2 P_R^2}{2_q(I_P + I_D)B + \frac{4kTB}{R_L} + \mathrm{RIN} \cdot I_D^2 B}.\end{aligned} \tag{50}$$

From Eq. (50), $P_R$ is the received optical power at the end of the optical link. On the other hand, in accord with Fig. 3 and Eq. (40), and by considering that the modulated optical power at the output of MZM is propagated through an optical fiber of length L, the $P_R$ can be written by $P_R = 10^{-\alpha_{\mathrm{fiber}} L/10} P_{\mathrm{out}}$. Here $\alpha_{\mathrm{fiber}}$ is the optical fiber loss, and L is the transmission distance of the optical fiber. In that case if we consider that $\pi \mathrm{Vm}/V\pi \ll 1$, then the Eq. (50) can be rewritten as:

$$\begin{aligned}\mathrm{SNR} &= \frac{\Re^2 (10^{-\alpha_{\mathrm{fiber}} L/10} P_{\mathrm{out}})^2}{2q(I_P + I_D)B + \frac{4kTB}{R_L} + \mathrm{RIN} \cdot I_D^2 B} \\ &= \frac{\Re^2 \left[\left(10^{-\alpha_{\mathrm{fiber}} L/10}\right) \frac{\alpha P_{\mathrm{in}}}{2} \left\{\frac{\delta^2}{2} - \delta\left[\frac{\pi V_m}{V_\pi}\right]\right\}\right]^2}{2q(I_P + I_D)B + \frac{4kTB}{R_L} + \mathrm{RIN} \cdot I_D^2 B}.\end{aligned} \tag{51}$$

This equation provides several insights into the SNR behavior of a receiver. Notice that as expected, increasing the optical power $P_{\mathrm{in}}$ increases the SNR. On the other hand, increasing the bandwidth of the receiver, $B$, reduces the SNR. The denominator of Eq. (51) shows the contribution of thermal noise, shot noise, and RIN to SNR. An interesting point is that as $R_L$ increases, the effects of thermal noise decrease. In a practical circuit, however, $R_L$ cannot be increased too much because it will reduce the bias headroom of the photodetector.

## 3 Experimental Results

According to the theoretical descriptions explained in Sec. 2, we assembled in the laboratory the proposed experimental setup shown in Fig. 5. For the stage at which relaxation oscillation frequencies were measured, we used two fiber-coupled DFB laser sources (Thorlabs, model S3FC1550) with a central wavelength of 1550 nm, a threshold current of ≈8 mA, and a differential responsivity of 0.25 mW/mA. An optical isolator OI was connected to each DFB laser to avoid instabilities by feedback into the lasers; an optical coupler was used to split the optical beam. In order to increase the power level of the microwave signal it was necessary to connect an optical fiber amplifier (EDFA) in one of the ports of the optical coupler. After that, the amplified optical signal was launched to fast photodetector PD1 (MITEQ model DR-125G-A), which has a typical optical to electrical transfer gain ($V/W$) of 1900 and −3 dB bandwidth of 12.5 GHz. In order to measure the optical spectrum of the DFB laser, it was necessary to connect the other one port of optical coupler to an optical spectrum analyzer (OSA; Anritsu model MS9710C). On the other hand, the obtained photocurrent by photodetector was measured by using an electrical spectrum analyzer (ESA; Agilent model E4407B). As can be seen from Fig. 6(a), the optical spectrum of one of the lasers DFB 1 exhibits sidebands on both sides of the main laser line as result of being biased in the threshold current region. In this case its optical power was emitted at 1.15 mW with a temperature of 23.5 °C. According to Eq. (24), the injection current was approximately at 12.6 mA. With these operation data, a microwave signal by using direct detection was obtained on C band, as shown in Fig. 6(b). This spectrum shows a microwave signal located at 4.17 GHz and its harmonic located at 8.34 GHz. This result is in good agreement with Eq. (30). Similar results were found with the laser DFB 2 when it was operated in the low laser threshold current region. Because of its linear relationship between relaxation oscillation frequency and the square root of the difference between the injection current and the threshold current as defined in Eq. (23), and since the optical power of each DFB laser can be tuned by using a power controller system, which modifies the injection current through laser diode correspondingly, we obtained several microwave signals located between 4 and 5 GHz for DFB 1, when it was tuned between 0.7 mW and 0.8 mW with a temperature of 25°C, as can be seen in Fig. 7(a). Microwave signal were obtained between 4.5 and 5.5 GHz, when the optical power of DFB 2 was tuned between 0.9 mW and 1 mW with a temperature of 26°C as can be seen in Fig. 7(b). To show a potential application in the field of communication systems of relaxation oscillation frequencies, we report in this paper the simultaneous multiplexed transmission of an analog TV signal of 67.25 MHz (TV channel 4) over a photonic link of 30 km of optical fiber by using two microwave signals at 4 and 5 GHz. From the experimental setup illustrated in Fig. 5, it can be seen that the obtained relaxation oscillation frequencies from the photodetector were mixed with a TV signal by using an electrical frequency mixer

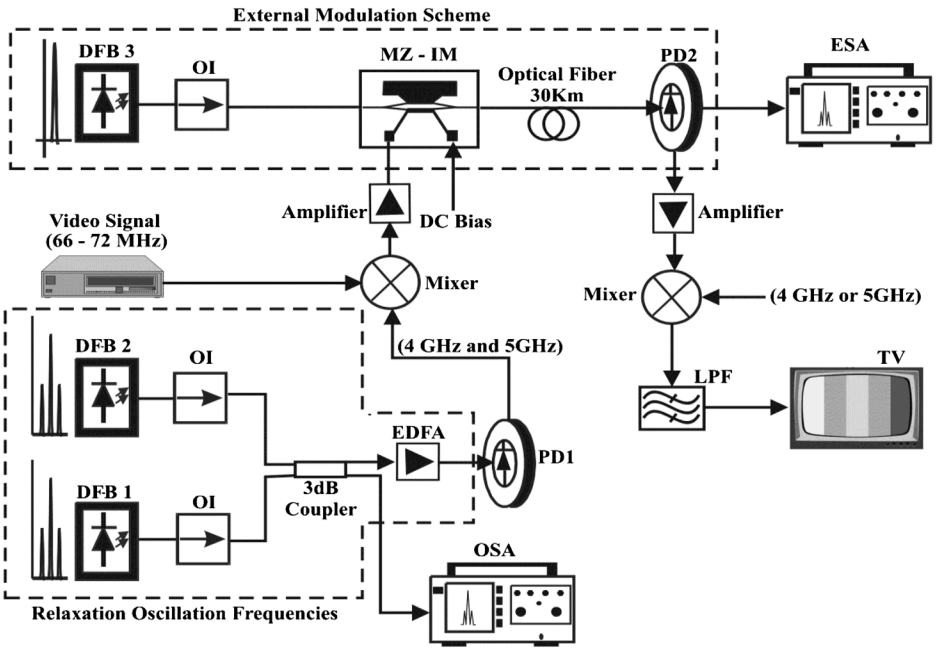


**Fig. 5** Experimental setup for transmitting a TV signal by using relaxation oscillation frequency as information carrier.

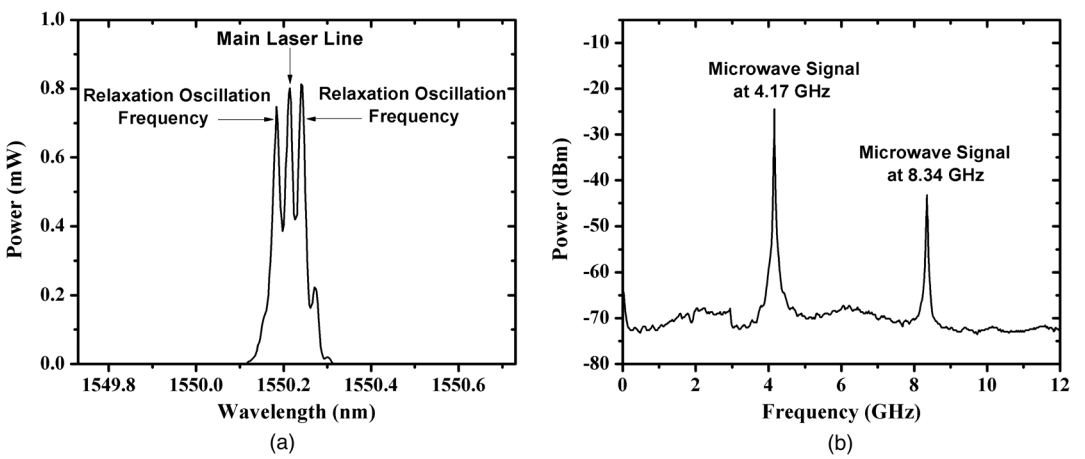


**Fig. 6** Measured spectrums: (a) showing relaxation oscillation frequencies, (b) microwave signal by using direct detection.

(Mini-Circuits, model ZX05-U72MH-s+). Then the obtained modulated signal, as shown in Fig. 8(a), was amplified and transmitted through a photonic link of 30 km of optical fiber. Such microwave sub-carriers were applied to an electro-optic modulator, which imprints the electric signal on the laser emission. The intensity-modulated optical signal of DFB 3 laser was then transmitted through the optical channel. After that, in the receiver, the transmitted information was photodetected. The spectrum of the multiplexed microwave signal after photodetection is shown in Fig. 8. The output electrical spectrums in Fig. 8 clearly show the multiplexed microwave sub-carriers. The spectral separation is approximately 1 GHz. According to the experimental setup shown in Fig. 5, the photodetected signal is amplified, filtered, and synchronously down-converted to recuperate the analog TV signal of 67.25 MHz. The resulting power spectral density was displayed in an electrical spectrum analyzer, where it was analyzed to measure the power level of recovered information. Figure 9(a) shows the frequency spectrum of an analog NTSC TV signal at the input of the transmitter located at 67.25 MHz (before being applied to frequency mixer). In Fig. 9(b), we can see the obtained analog NTSC TV signal at the output of the receiver when the local oscillator was synchronized at 4 GHz. The analog information was successfully transmitted from the transmitter to the receiver, and the received signal was satisfactorily reproduced at the receiver without noticeable degradation compared to the original NTSC TV signal. In order to measure the quality of the received signal, it was necessary to quantify experimentally the parameter of SNR for both cases (TV transmitted and recovered in the photonic link). Figure 10(a) shows the frequency spectrum of the original NTSC TV signal before being transmitted through 30 km of optical fiber. As can be seen from this figure, the SNR measured in a bandwidth of 6 MHz was of 52.67 dB. On the other hand the SNR measured in the receiver was of 46.5 dB, as shown in Fig. 10(b). Notice that the SNR measured in the receiver was degraded by 6.17 dB due to the

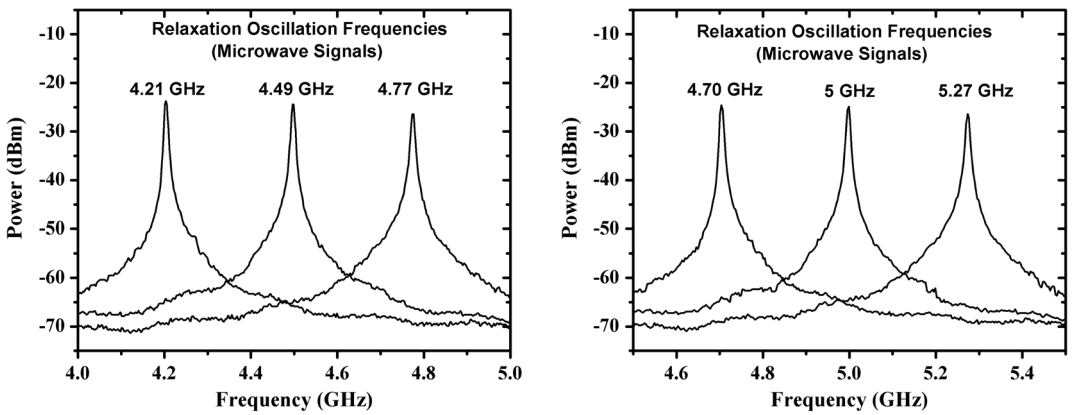


**Fig. 7** Microwave signal continuously tuned: (a) between 4 and 5 GHz, (b) between 4.5 and 5.5 GHz.

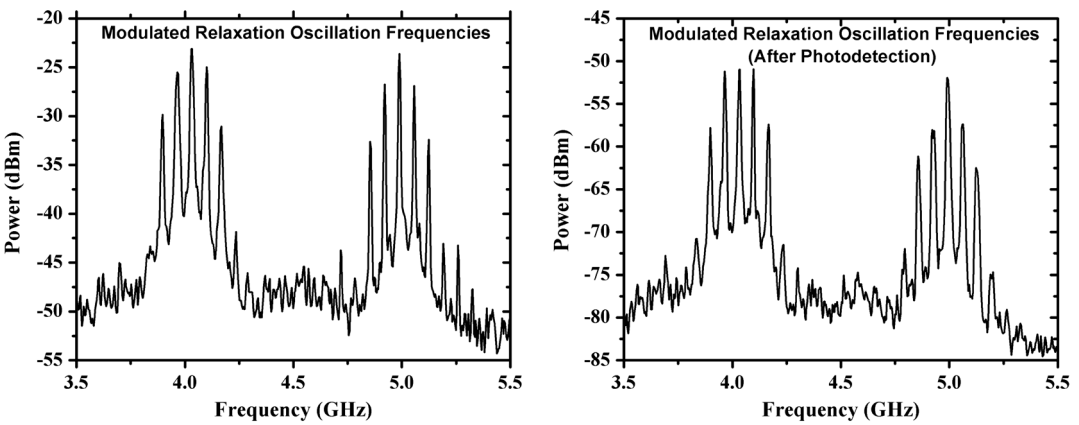


**Fig. 8** Modulated relaxation oscillation frequencies with a TV signal: (a) applied to electro-optic modulator, (b) after photodetection.

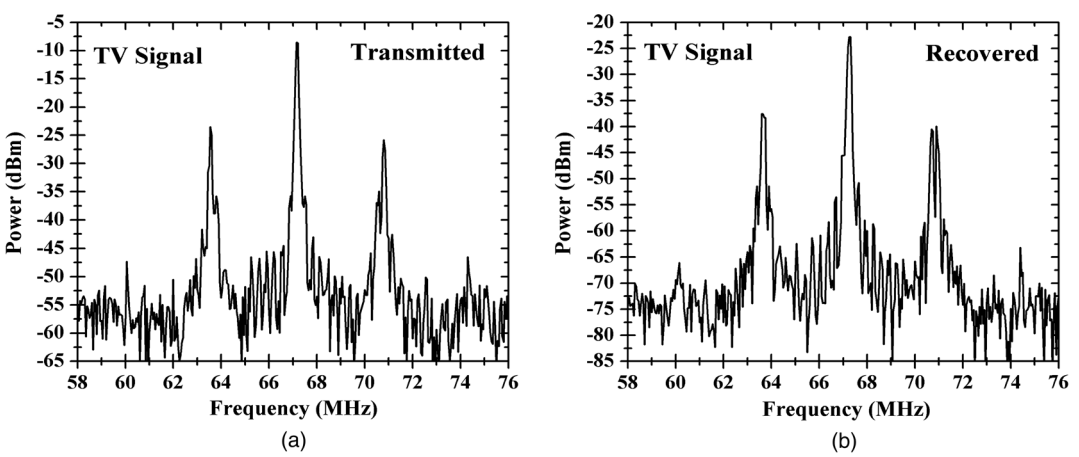


**Fig. 9** TV signals at 67.25 MHz: (a) transmitted, (b) recovered.

optical fiber loss, and it could be improved substantially with the addition of another stage of electrical amplification at the end of the link. However, values of SNR 45 dB ensure good images quality.[20] The differential gain and differential phase were not measured in this paper. Nevertheless, we have experimentally demonstrated that the generated microwave signals (relaxation oscillation frequency) by using direct detection can be used as information carriers in a multiplexed transmission system based in an analog photonic link, and we have used a test of TV signal to verify it.

## 4 Discussion

1. Generally, RoF systems transmit an optically modulated RF signal from a central office (CO) to a base

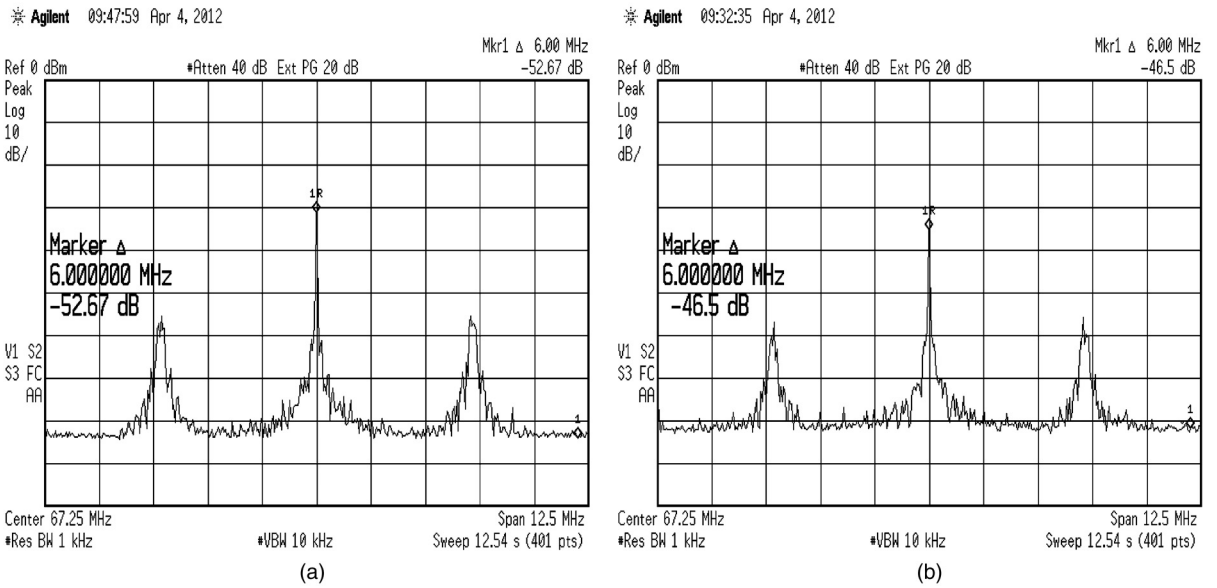


**Fig. 10** TV signals at 67.25 MHz in order to measure experimentally the SNR parameter: (a) transmitted, (b) recovered.

station (BS) via an optical fiber. The RF signal recovered using a photodetector at the BS arrives at a user terminal (UT) through a wireless channel. This architecture provides a cost-effective system, since any RF oscillator is not required at the BS. However, the performance of RoF systems depends on the method used to generate the optically modulated RF signal.[21] Microwave signal generation by optical means is a technique that has several advantages over conventional electronic techniques, such as high frequency and wide frequency tenability, as well as offering better flexibility and immunity to electromagnetic interferences. In addition, due to the extremely low loss of the state-of-the-art fibers, a microwave signal can be distributed over an optical fiber over a long distance. In general, photonic generation of microwave signals can be divided into three categories.

(a) In the first category, two laser beams from two different laser sources are applied to a photodetector. A beat signal with a frequency equivalent to the spacing of the two wavelengths is obtained at the output of the photodetector. To generate a signal with low phase noise and high stability, the phases of the two laser sources must be locked, which is usually implemented by using optical injection locking or by an optical phase-locked loop. For both methods, a high-quality microwave reference signal is required.[22] However, these approaches are expensive and complicated.[23]

(b) In the second category, microwave signals are generated on the basis of external modulation technique. The external modulator can be either an electro-optic intensity modulator or a phase modulator. A key advantage of these approaches is that frequency-doubled or -quadrupled signals can be generated with a relatively low-speed external modulator. However, similar to the approaches in the first category, a high-quality microwave reference source is required.[23]

(c) To avoid using a reference microwave source, in the third category, microwave or millimeter-wave signals are generated by using a single laser source. To obtain a beat signal at the output of a photodetector, the laser source should have either a single wavelength with dual longitudinal modes or two wavelengths operating in single longitudinal mode (SLM) for each wavelength. The beating of the dual longitudinal modes or the two SLM wavelengths would generate a microwave signal with the required frequency.[23]

2. On the other hand, next-generation wireless systems are likely to use bands below 6 GHz, where radio propagation characteristics are suitable for low-cost network deployments, although higher frequencies may be preferred in some cases due to greater spectrum availability. If higher frequencies are used, for example the mm-wave bands, fiber dispersion can become a serious problem even over relatively short spans for conventional double sideband modulation.[24]
3. In this paper we have used two DFB laser diodes emitting at 1550 nm and operating in the low laser threshold current region. When the emissions generated in both lasers are combined with an optical fiber coupler and detected by a fast photodetector using direct detection method, two microwave signals are obtained. This alternative method to generate microwave signals does not need a high-quality microwave reference source. The main contribution of this work resides on the research about the use of DFB lasers operating in the low laser threshold current region. To our knowledge is the first time that a work demonstrating a practical application using this technique is reported.

4. It is true that the electro-optical system presented in this work requires precise control in terms of electricity and temperature; however, we considered this technique an interesting technological alternative, taking into account that it is practically all-optical, and consequently unnecessary loss and electrical noise due to optical-to-electrical ($O/E$) conversion and electrical-to-optical ($E/O$) conversion are avoided.[25] The unique electro-optical conversion is placed at the output of the photodetector. The use of an EDFA allows that microwave electrical signals to be generated on the optical domain without an additional electrical amplification stage. Besides, the authors consider that the main advantage in terms of cost effectiveness lies in that it is possible to transmit analog information using only a laser diode to generate microwave signals in the transmitter and it can be used as optical carrier in the external modulation scheme shown in Fig. 5.
5. On the other hand, it is well known that currently, researches on RoF systems are a topic of interest because of the great advantages that this represents in the area of telecommunications. In this sense, an interesting alternative for our work here reported could be done if at the output of the PD1 as shown in Fig. 5 an electrical combiner is placed, and in this way the resultant signal could be radiated by using an antenna. At the end of the optical link and by using another antenna the demodulated signal could be recovered, and by consequence our work here proposed could operate as an all RoF system. A prototype for the setup here explained was successfully demonstrated in Ref. 26.

## 5 Conclusions

In this paper we have experimentally demonstrated that two DFB lasers biased in the low laser threshold current region showed relaxation oscillation frequencies in the laser intensity. These frequencies were seen as sidebands on both sides of the main laser line when the optical spectrum was analyzed with a spectrum analyzer. This result allowed the generation of microwave signals on C band by using the operation principle of direct detection. In addition to the proposed experimental setup in this work, an analog NTSC TV signal was simultaneously transmitted in an analog photonic link by using relaxation oscillation frequency as information carriers located at 4 and 5 GHz. The signal TV was received satisfactorily when the local oscillators were synchronized in the receiver. For our proposed experimental setup to recover the transmitted information successfully, it was necessary to have additional amplifiers that adapt the power levels, improving the quality of the signals. The results obtained in this work ensure that as an interesting alternative, several modulation schemes can be used for transmitting not only analog information but also digital information by using relaxation oscillation frequencies as information carriers. As proposed experimental setup described here can generate microwaves continually tuned, we can use this feature to transmit several TV signals using frequency division multiplexing schemes (FDM) and wavelength division multiplexing (WDM) techniques, not only point to point but also by using bidirectional systems, exploiting the use of mature microwave signal processing techniques, where multiple signals are multiplexed in the microwave domain and transmitted by a single optical carrier when sub-carrier multiplexing (SCM) schemes are proposed. To the best of our knowledge, this is the first published work on the employment of relaxation oscillation frequencies as information carriers for transmitting analog TV signals on a long-distance photonic link. Besides as an alternative of analog photonic links, our proposal shows an outstanding performance.

### Acknowledgments

This work was supported by The Mexican Consejo Nacional de Ciencia y Tecnología (CONACyT), (Grant No. 102046).

### References

1. K. Wang et al., "A radio-over-fiber downstream link employing carrier-suppressed modulation scheme to regenerate and transmit vector signals," *IEEE Photon. Technol. Lett.* **19**(18), 1365–1367 (2007).
2. D. Novak et al., "Fiber-radio-challenges and possible solutions," presented at the *Int. Topical Meeting Microwave Photonics 2003*, pp. 49–54, IEEE Xplore (Sep. 10–12 2003).
3. X. Zhang et al., "A novel millimeter-wave-band radio-over-fiber system with dense wavelength-division multiplexing bus architecture," *IEEE Trans. Microw. Theory Tech.* **54**(2), 929–937 (2006).
4. S. Iezekiel, *Microwave Photonics Devices and Applications*, John Wiley (2009).
5. X. J. Meng, "A dispersion tolerant analog optical receiver for directly modulated RF photonic links," *IEEE Photon. Technol. Lett.* **19**(6), 438–440 (2007).
6. S. Mikroulis et al., "Evaluation on the performance of distributed feedback lasers (DFB) for radio-over-fiber (RoF) applications," in *Int. Conf. on Telecommunications & multimedia*, pp. 1–8, 2006© Research and Development of Telecommunications Systems Laboratory, Greece (2006).
7. A. Baylón-Fuentes et al., "Modulation of relaxation oscillation frequency of a DFB laser by using direct detection," *Proc. SPIE* **7958**, 79580E (2011).
8. A. García-Juárez et al., "Analog photonic link by using DFB lasers operated in the low laser threshold current region and external modulation," *Proc. SPIE* **8282**, 828201 (2012).
9. H. Zandi et al., "Analysis of power harmonic content and relaxation resonant frequency of a diode laser," *Proc. SPIE* **6468**, 64680J (2007).
10. H. Zandi et al., "Harmonic content and relaxation resonant frequency of a modulated laser diode," *Trans. D: Comput. Sci. Eng. Elect. Eng.* **16**(2), 145–156 (2009).
11. M. Bavafa et al., "Optimal operation point for the primary harmonic content of a modulated laser diode," in *Proc. 6th WSEAS International Conference on Microelectronics, Nanoelectronics, Optoelectronics*, pp. 86–91, WSEAS E-Library, Istanbul, Turkey (May 27–29 2007).
12. L. A. Coldren and S. W Corzine, *Diode Lasers and Photonic Integrated Circuits*, John Wiley & Sons (1995).
13. B. E. A. Saleh, *Fundamentals of Photonics*, pp. 624–626, John Wiley & Sons, Inc. (1991).
14. D. Derickson, *Fiber Optic Test and Measurement*, pp. 175–179, Prentice Hall PTR (1998).
15. C. H. Cox, *Analog Optical Links: Theory and Practice*, Chapter 2, pp. 37–38, Cambridge University Press, Cambridge (2004).
16. X. Meng Jun and A. Karim, "Microwave photonic link with carrier suppression for increased dynamic range," *Fiber Integrated Opt.* **25**(3), 161–174 (2006).
17. E. Garmire, "Sources, modulation, and detectors for fiber-optic communication systems," in *Fiber Optics*, Handbook, Edited by M. Bass, pp. 4.1–4.78, McGraw-Hill, New York (2002).
18. L. Kazovsky, S. Benedetto, and A. Willner, *Optical Communications Systems*, Artech House (1996).
19. A. Joshi et al., "Balanced photoreceivers for analog and digital fiber optic communications," *Proc. SPIE* **5814**, 39–50 (2005).
20. M. Kowalczyk and J. Siuzdak, "Multi-channel am video transmission beyond the baseband of multimode fiber," *Microw. Opt. Technol. Lett.* **52**(2), 435–438 (2010).
21. T.-S. Cho et al., "Analysis of CNR penalty of radio-over-fiber systems including the effects of phase noise from laser and RF oscillator," *J. Lightwave Technol.* **23**(12), 4093–4100 (2005).
22. X. Chen, Z. Deng, and J. Yao, "Photonic generation of microwave signal using a dual-wavelength single-longitudinal-mode fiber ring laser," *IEEE Trans. Microw. Theory Tech.* **54**(2), 804–809 (2006).
23. M. Qasymeh, W. Li, and J. Yao, "Frequency-tunable microwave generation based on time-delayed optical combs," *IEEE Trans. Microw. Theory Tech.* **59**(11), 2987–2993 (2011).

24. D. Wake, A. Nkansah, and N. J. Gomes, "Radio over fiber link design for next generation wireless systems," *J. Lightwave Technol.* **28**(16), 2456–2464 (2010).
25. H. Kosek et al., "All-optical demultiplexing of WLAN and cellular CDMA radio signals," *J. Lightwave Technol.* **25**(6), 1401–1409 (2007).
26. P. Hernndez-Nava et al., "Microwave hybrid fiber-radio system based on optical heterodyne technique," in *Proc. of the Information Photonics Conf.*, pp. 18–20, IEEE Xplore, Ottawa, Canada (May 2011).

**Alejandro García Juárez** received his BS degree in electronics engineering from Universidad Autónoma de Puebla, México, in 1998, and his MS and PhD degrees in optics with specialty in optoelectronic systems from the Instituto Nacional de Astrofísica, Óptica y Electrónica, Tonantzintla, México in 1999 and 2005, respectively. He is currently a titular professor-researcher with Department of Research in Physics of the Universidad de Sonora, México. His current research interests are primarily in fiber optics communication systems and microwave photonics. He is a member of SPIE.

**Ignacio E. Zaldivar-Huerta** received his BS degree in electronics engineering from Universidad Autónoma de Puebla (México) in 1992, his MS degree in microelectronics from the Instituto Nacional de Astrofísica, Óptica y Electrónica (México) in 1995, and his PhD degree in sciences for the engineering from Université de Franche-Comté (France) in 2001. Since February 2002, he has been with the Department of Electronics of the Instituto Nacional de Astrofísica, Óptica y Electrónica in Tonantzintla, Puebla, México. Currently he is a titular researcher. He has authored or co-authored more than 15 conferences and journal publications. His current research interests are primarily in fiber optics communication systems, and electro-optic devices on silicon. He is a member of IEEE and SPIE.

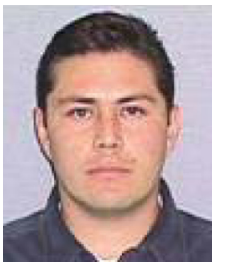

**Jorge Rodríguez-Asomoza** received his BS degree in electronics and his MS degree in optoelectronics from the Benemérita Universidad Autónoma de Puebla (BUAP), México, in 1996 and 1997, respectively. In April 2001, he received the PhD degree from the National Institute of Astrophysics, Optics, and Electronics (INAOE), in Tonantzintla Puebla, México. Since August 2001, he has been a titular Professor at the Department of Electrical Engineering of Universidad de las Américas, Puebla, where he works with optical modulators for electric signal sensing systems, optical communications systems, and signal processing.

**María del Rocío Gómez Colín** received her BS degree in electronics engineering from Instituto Tecnológico de Oaxaca, México, in 1997, and her MS degree in optics with specialty in optoelectronic systems from the Instituto Nacional de Astrofísica, Óptica y Electrónica, Tonantzintla, México in 2001. She is currently an associate professor-researcher with Department of Physics of the Universidad de Sonora, México. Her current research interests are primarily in optoelectronic systems and holography.